atmosphere

Article

Influence of Local Climate and ENSO on the Growth of *Cedrela odorata* L. in Suriname

Michael Köhl *, Neda Lotfiomran and Archana Gauli

Institute of Wood Science-World Forestry & Center for Earth System Research & Sustainability (CEN), University of Hamburg, Leuschner Strasse 91, D-21031 Hamburg, Germany; neda.lotfiomran@uni-hamburg.de (N.L.); archana.gauli@uni-hamburg.de (A.G.)
* Correspondence: michael.koehl@uni-hamburg.de

Abstract: In this study, we used retrospective dendroclimatological analyses to explore whether El Niño Southern Oscillation (ENSO) and local precipitation patterns have an influence on tree growth in Suriname, a country located on the Guiana Shield, as annual precipitation patterns on the Guiana Shield are related to ENSO. Discs were taken from 20 trees of *Cedrela odorata*, whose stem forms very distinct annual growth rings, for tree ring analyses. The trees grew in unmanaged tropical wet forests of Suriname. The tree-ring series of individual trees started between 1836 and 1931 and extended over a period of 84–180 years. The 20 dated series were utilized for constructing a tree-ring chronology. Unlike many other studies that used local anomalies such as flood pulse, precipitation, and drought events to describe the influence of El Niño on tree growth, we used monthly precipitation and ENSO indices as predictors of tree growth to calculate response and correlation functions. The study observed that tree ring growth of *Cedrela odorata* is influenced by precipitation in August and June of the current year and in August of the previous year, as well as by the ENSO indices SSTA, TSA, TNA, and NAO. Systematic increases in the strength of the El Niño southern oscillation (ENSO) teleconnection due to climate change could affect the growth of trees on the Guiana Shield.

Keywords: dendroclimatology; neotropic; *Cedera odorata* L.; climate–growth relationship; global climate change; ENSO

check for updates

Citation: Köhl, M.; Lotfiomran, N.; Gauli, A. Influence of Local Climate and ENSO on the Growth of *Cedrela odorata* L. in Suriname. *Atmosphere* **2022**, *13*, 1119. https://doi.org/10.3390/atmos13071119

Academic Editor: Álvaro Enríquez-de-Salamanca

Received: 15 June 2022
Accepted: 14 July 2022
Published: 15 July 2022

1. Introduction

End-of-century projections indicate declines in rainfall in the Caribbean and the Guiana Shield during the rainy seasons under the IPCC SRES A1B scenario [1]. Located along the northern coast of South America, the Guiana Shield encompasses 40% of the total area of the Amazon biome. It underlies French Guiana, Suriname, Guyana, Venezuela, and parts of Colombia and Brazil. The long-distance effects of El Niño Southern Oscillation (ENSO) on the climate of the Guiana Shield will most likely undergo modifications, as climate change will have impacts on the physical processes associated with ENSO [2,3]. Nurmohamed et al. [4] showed in a statistical analysis of the rainfall in Suriname that "rainfall correlates well with sea surface temperature anomalies (SSTAs) in the tropical North Atlantic (TNA), the tropical South Atlantic (TSA), Niño 1 + 2, Niño 3 .4, Atlantic Niño, and the tropical Atlantic (TA) dipole region". El Niño-related effects on freshwater and brackish-water fishes have already been reported for Suriname [5]. Iizumi et al. [6] highlighted the importance of ENSO for global crop production. The effects of El Niño climate change on forest resources tend to be less dramatic than for annual crops due to the longevity of trees. However, the sensitivity of tree growth toward climatic factors and El Niño Southern Oscillation (ENSO) has been reported among others for Ethiopia, Panama, Peru, Ecuador, Brazil, Chile, Argentina, Spain, Mexico, Columbia, Costa Rica, DRC, and the Amazonian floodplains [7–19]. Tree growth alterations caused by climate change could impact growth-dependent concurrence and species abundances on the Guiana Shield.

The investigation of climatic influences on the growth of trees requires long-term time series with annual resolution. Long-term studies with the repeated recording of individual trees have been carried out in temperate and boreal forests for more than 100 years [20–22], but are rare on the Guiana Shield. Dendrochronological methods, which allow retrospective analysis of tree growth on the basis of tree rings, offer an alternative for such studies. Dendroclimatology studies explore the relationship between annual tree growth and climate. Climate-related tree-growth attributes such as tree-ring width, wood density, or isotopic measurements can be utilized for the quantitative analysis of former climatic patterns [23,24]. As the climate signal is confounded by many other factors that are not related to climate such as tree species, tree age, management, concurrence, soil nutrient characteristics, pests, or exposure to sunlight, the climate signal needs to be separated from the remaining "background noise" [23]. This is commonly achieved by deriving a tree-ring chronology from available individual tree-ring series, which allows identifying climate signals that affect the growth pattern of trees.

Retrospective dendroclimatological analyses can provide valuable indications for future tree growth under climate change [18,25–27]. While, in temperate and boreal forests, the effects of future changes in annual temperature and precipitation patterns, as well as the length of drought periods, on tree growth are discussed intensively [28,29], comparatively few studies are found in tropical and subtropical forest ecosystems. The reason for the few studies might be due to the unavailability of long-term tree growth data, and climatic records covering more than a century are rare. Natural tropical forests are by far more heterogeneous than boreal and temperate forests [30–33], and trees growing in unmanaged, heterogenic tropical forests show distinct growth variability caused by neighboring effects [34,35], which make it less preferred for dendroclimatological study. Moreover, the supply rate of required resources (light, nutrients, water, and edaphic conditions), changing balance between photosynthesis and respiration, increased hydraulic resistance, decreased nutrient supply, or genetic changes with meristem age [36–41], as well as the formation of tree rings in tropical trees, is complex and can be observed only for a limited number of tree species and climatic conditions [42,43], further hindering dendroclimatological study.

We apply the methods of dendroclimatology to retrospectively investigate possible climate–growth relationships for trees of the Guiana Shield. In addition to monthly climate data, we use parameters describing ENSO effects for the dendroclimatological analyses. We investigate the impacts of local climate and ENSO effects on the growth of the tree species *Cedrela odorata*. This provides important insights into tree growth under future climate change for this region.

2. Materials and Methods

2.1. Study Site

Suriname is located in the northeast of South America between latitudes 1° and 6° N and longitudes 54° and 58° W. About 95% (153,320 km^2) of Suriname's land area is covered by natural tropical rainforests [44]. Suriname exhibits a low deforestation rate and is characterized as a country with high forest cover and low deforestation (HFDL). Suriname was selected for this study because it is located in the center of Guiana Shield, and a link has been established between precipitation patterns and ENSO [4]. The study was conducted in the central part of the natural rainforest belt in Suriname (5°22′ N, 55°55′ W) (Figure 1). Trees used for the study came from legal commercial harvests on logging concessions in natural forests granted by the Surinamese government. In accordance with the Forest Management Act of 1992, the concessions are subject to sustainable forest management.

Figure 1. Map of Suriname showing the sample collection site and the metrological station, Zanderij. The square shows the origin of the samples.

2.2. Climate Data

According to Köppen–Geiger's classification, Suriname has a tropical rainforest climate (Af) with an average annual temperature of 27.5 °C and an average humidity of 80–90%. Between day and night, the temperature fluctuates about 10 °C around the average daily temperature. The average annual precipitation is about 2200 mm. Climate diagrams show a clear seasonality, with a short, wet season from December to January, the beginning of a long, wet season from March to May, the end of the long, wet season from June to August, and a dry season from September to November (Figure 2) [4]. The seasonal cycle of the monthly rainfall is caused by the meridional movement of the Intertropical Convergence Zone (ITCZ). In Suriname, there are distinct regional differences in climate. The inland regions are hotter and wetter in contrast to the coast where the climate is cooler and dryer [45]. According to Nurmohamed, Naipal, and Becker [4], precipitation is highest in the mountainous area in the center of Suriname (~2800 mm) and lowest in the low altitudes in the northwest (~1650 mm). Twelve rainfall gauge stations are located in Suriname. For our study, we utilized precipitation data that were collected by the Meteorological Service Suriname (MDS) from the meteorological station in Zanderij, which is located closest (~50 km) to the study site.

ENSO data were obtained from the Met Office Hadley Center's sea ice and sea surface temperature (SST) dataset [46]. As ENSO is a large, complex, and dynamic system, several indices have been developed that use different combinations of attributes such as air pressure or sea surface temperature of different regions. The website hosted by the Global Climate Observing System (GCOS) Working Group on Surface Pressure (WG-SP) gives detailed explanations of the indices (www.esrl.noaa.gov/psd/gcos_wgsp/Timeseries, accessed on 14 June 2022). We accessed this website to download the datasets Niño 3 .4 (1870–May 2017), Niño 1 + 2 SST Index (1870–May 2017), Multivariate ENSO Index (MEI, 1950–2017), Southern Oscillation Index (SOI, 1866–2016), and North Atlantic Oscillation

Index (NAO, 1821–2015). NAO was included, as it has a remote influence through the Hadley circulation on the sea surface temperature anomalies (SSTAs) [4].

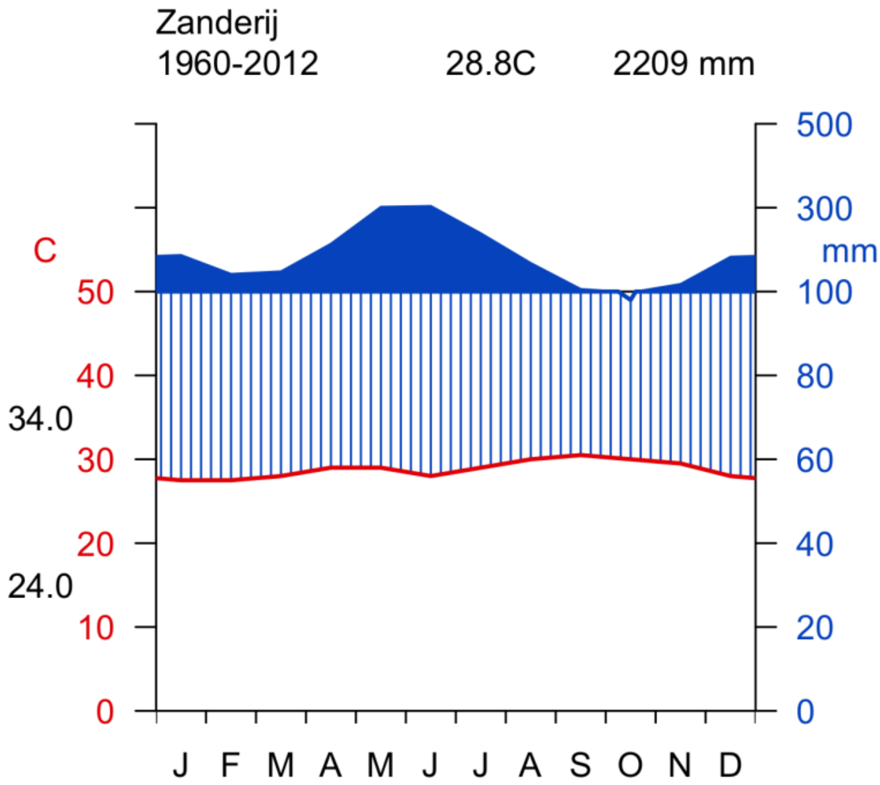

Figure 2. Walter–Lieth climate diagram for metrological station in Zanderij, Suriname. The precipitation and temperature data were measured from 1960 to 2012. The left *y*-axis shows the temperature (°C), while the right *y*-axis shows the precipitation (mm). The *x*-axis shows the months. The red curve shows the temperature, while the blue curve shows the precipitation. The climate diagram was created by the R package Climatol [47].

2.3. Tree Species

Due to very distinct annual growth rings, the tree species Cedro Hembra (*Cedrela odorata* L.) was chosen [43]. *C. odorata* is a deciduous, monoecious (male and female flowers are borne on the same inflorescence) and medium-sized to large tree of the Meliaceae family. The timber of large, mature trees is considered very valuable and is one of the world's most important commercial timber species. *C. odorata* is widespread but never very abundant throughout moist tropical American forests; its numbers are continuing to be reduced by exploitation without successful regeneration [47]. The International Union for the Conservation of Nature (IUCN) listed *C. odorata* as a vulnerable tree species [48]. *C. odorata* develops best in seasonally dry climates, as reflected by its deciduous habit which leads to the formation of growth rings [47]. In Suriname, *C. odorata* flowering occurs at the end of the rainy season, and leaves are thrown during the long, dry season.

The annual nature of ring formation in South America has been proven in several studies [25,43,49,50]. The wood anatomy structure of *C. odorata* shows distinct growth ring boundaries and ring porosity, characterized by fiber bands and vessel bands embedded in the paratracheal parenchyma (Figure 3). The main dry season with rainfall well below 100 mm is likely to lead to the annual formation of tree rings [51].

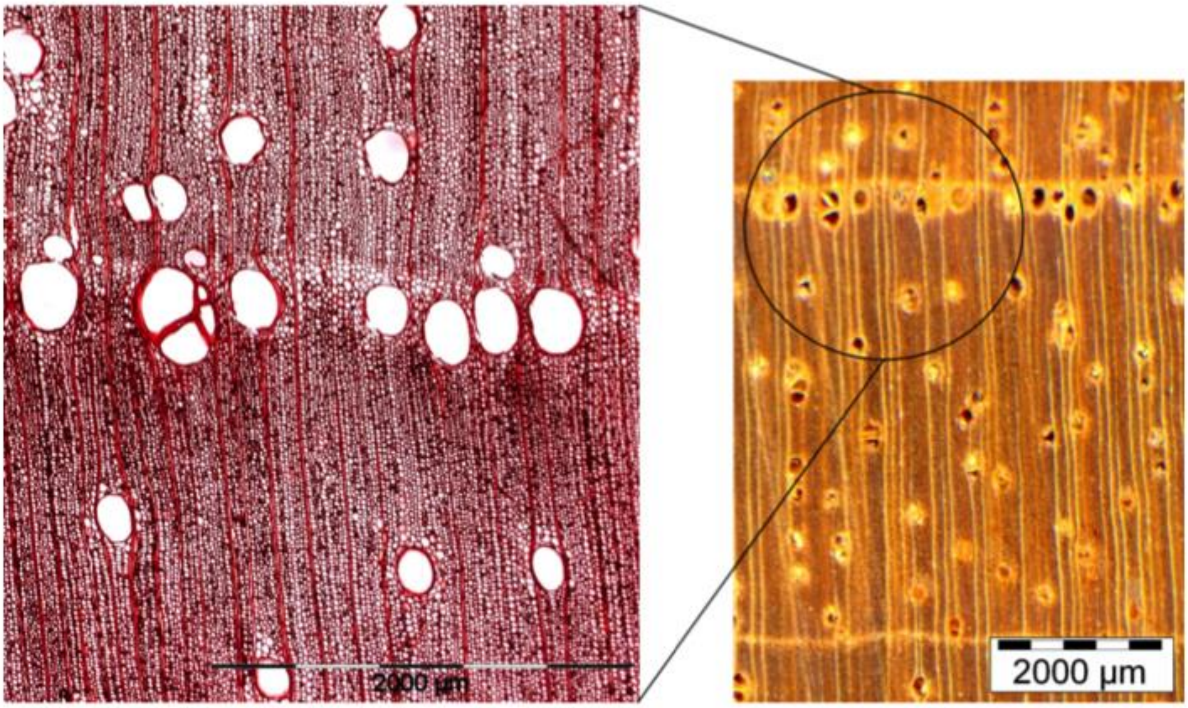

Figure 3. Microsection (**left**) and tree-ring boundaries (**right**) of *C. odorata*.

2.4. Sample Selection

Between 2014 and 2015 a total of 145 trees of the species *C. odorata* were legally harvested in Suriname according to Suriname's national record of logged trees. From these 145 trees, we randomly selected a sample of 20 trees and extracted cross-sectional wood discs at the lower (i.e., thicker) end of the logs. All the samples were taken from above the buttresses (about 2 m above from the ground). The diameter of the trees varied from 41 cm to 79 cm. With legal approval issued by the Suriname's Foundation for Forest Management and Production Control (SBB), the discs were shipped to Hamburg, Germany, for further analyses.

2.5. Tree-Ring Measurement

After the samples were air-dried to avoid fungal attack, they were polished mechanically with increasingly finer sandpaper (up to grain of 1000). On the sanded discs, wedging rings and discontinuous rings (the rings which occurred only over the part of the disc) were detected by marking each ring and interconnecting every tenth ring between the different radii to reduce errors. For trees with several multiple wedging rings, those radii were chosen which corresponded best to the average diameter of the disc. At least four radii were selected, and tree-ring boundaries were marked under binoculars. Every tenth ring was interconnected between radii to verify the correctness of marking. The widths of the individual annual growth rings were measured to the nearest 0.01 mm and digitized using a moving table LINTAB [52]. Before the tree-ring measurements were utilized for further analyses, they underwent extensive validation procedures in order to detect apparent measurement errors, such as missing or false tree rings. For the validation, we used the TSAP-Win software [53], which allows for cross-dating the time series within individual trees and among the entire set of trees. The procedure checks the growth patterns of individual trees for similar characteristics which can be synchronized and assigned to a distinct year of wood formation [54]. Following the good practice in dendrochronology, several statistics were computed to describe the key properties of a site chronology, described as follows:

(1) The mean intertree correlation (rbt), which is calculated as the mean correlation between all possible pairs of individual series for the entire series or by using the windowing technology for a sequence of overlapping time intervals through the entire length of the chronology strength of the signal common to all trees [55];
(2) The first-order autocorrelation (AC) within the series, which describes the influence of the previous year's conditions on ring formation [23];
(3) The expressed population signal (EPS), which quantifies the degree to which the chronology expresses the population chronology [56];
(4) The degree of synchronicity (Gleichläufigkeit), which is a classical agreement test based on sign tests between the pairwise comparison of all records in a dataset for the conformity of slopes between successive years [57];
(5) The t-value based on 5 year moving averages for the estimation of the cross-correlation between the sample and the reference [58].

The raw tree-ring series were checked for measurement errors with the software COFECHA [59] and the R-package dplR [60], which calculate correlation coefficients between individual tree-ring series to identify missing and false rings.

2.6. Chronology Construction

Climate is one among a variety of factors that influence tree growth. In order to extract the climate signal from tree-ring series, those other factors have to be removed as best as possible, which is commonly realized by detrending. Bunn et al. [60] described detrending as "the estimation and removal of the low-frequency variability that is due to biological or stand effects". We removed long-term growth trends from the raw measurements by applying a cubic spline with a frequency response of 0.5 at a wavelength of 0.67 times the series length. For trees from closed-canopy stands, spline functions are the most appropriate method for detrending tree-ring series [25,61]. Standardization was performed by calculating the dimensionless ring-width index (rwi), which results from dividing each series by the growth trend. On the basis of the detrended and standardized tree-ring series, a residual master chronology was built by averaging across the years utilizing the residuals of an AR process [60]. For each tree-ring series, the correlation with the master series was calculated. The correlations were performed for 50 year segments, and segments lagged by 25 years. All calculations were realized by the R-package dplR [60,62,63].

2.7. Dendroclimatological Analysis

Dendroclimatological analyses focus on the detection of relationships between annually resolved tree-ring data and climatic data, which usually show monthly resolution. These relationships can either be calculated as correlation functions that are mainly based on Pearson's linear correlation estimates or as response functions that apply indirect regression techniques. Climatic data are subject to multicollinearity, which limits the application of simple correlation and regression techniques. An alternative to deal with multicollinearity is offered by principal component regression techniques that regress the proxy record against principal components of climatic data. Zang and Biondi [59] implemented this approach in the R-package "treeclim". The regression is performed against principal components of an orthogonalized design matrix. Principal components are retained according to the cumulative eigenvalue product [64]. After the estimated regression coefficients are transformed into the original parameter space, Pearson's linear correlation is computed between the response variable and the climate data [65]. To test for significant correlations, bootstrap resampling with 1000 iterations is applied. Zang and Biondi [66] gave further details on the statistical procedures implemented in the R-package "treeclim".

3. Results

3.1. Tree-Ring Chronology

The 20 dated series with 2751 measurements in total (Figure 4) were utilized for constructing the tree-ring chronology. The tree-ring series of individual trees started between 1836 and 1931, extending over a period of 84 to 180 years, with an average time length of 137.55 years. The mean annual radial increment between the trees varied from 0.12 cm to 0.27 cm with an overall average of 0.2 cm. The series had a mean series intercorrelation of 0.353 and a mean first-order autocorrelation of 0.066 (SD = 0.135), which shows that the annual ring growth is subject to pronounced fluctuations. The degree of synchronicity (Gleichläufigkeit) between all pairwise combinations of trees ranged between 0.49 and 0.86 with an overall mean of 0.65, indicating a moderate agreement of the direction of slopes between adjacent years among the tested tree-ring series.

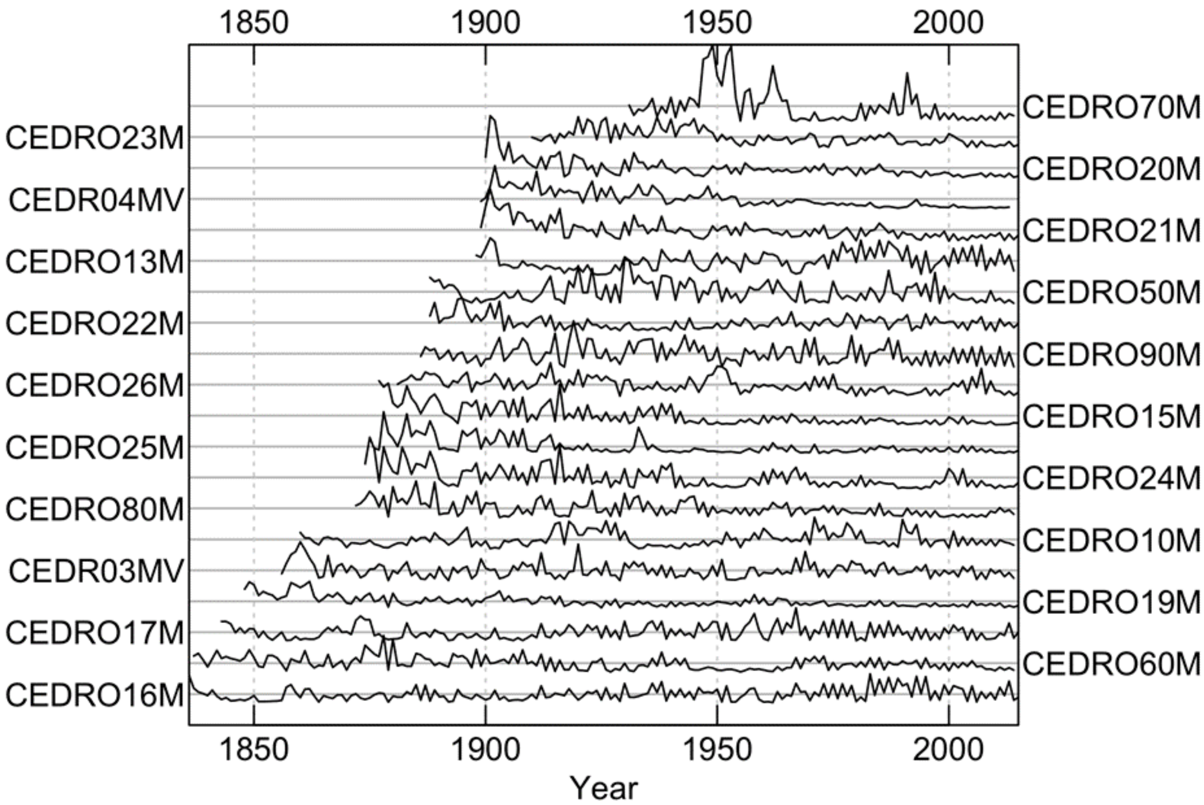

Figure 4. Tree-ring series of the 20 samples.

The first step of the statistical analysis was to check the quality of the 20 tree-ring series in order to detect measurement errors, such as interannual growth zones or wedging rings. For this purpose, we detrended and standardized the tree-ring series [62,67]. Detrending removes the variation of tree-ring width corresponding to biological growth trends and certain growth disturbances from the tree-ring series, which was achieved via pre-whitening, which adds the residuals of an AR model to the series mean. A master series was derived from all series, and then the correlation with the master series was calculated for each series. The analyses were conducted using the R-package diplR [60,62].

The correlation of each series with the master series is presented in Table 1 for time segments of 50 years. Nonsignificant correlations were observed for three segments (CEDRO16M: 1875–1924; CEDRO17M: 1875–1924; CEDRO4MV: 1925–1974). In dendrochronology, it is good practice to remove tree-ring series that show low correlations with the master series to maximize the common signal of the series used for building the chronology [25,68]. We decided not to truncate the tree-ring series by eliminating series with low correlations. This maintains the variability of tree growth and results in conservative estimations of climate–growth relationships [27].

Table 1. Correlation (Spearman's rho) of tree-ring series with master series.

Tree	1850–1899	1875–1924	1900–1949	1925–1974	1950–1999	Overall
CEDRO16M	0.62	0.21	0.34	0.49	0.30	0.39
CEDRO60M	0.67	0.53	0.36	0.32	0.47	0.52
CEDRO17M		0.19	0.26	0.50	0.32	0.29
CEDRO19M	0.73	0.60	0.63	0.53	0.49	0.65
CEDR03MV		0.26	0.39	0.49	0.45	0.39
CEDRO10M		0.25	0.23	0.44	0.49	0.40
CEDRO80M			0.62	0.57	0.48	0.52
CEDRO24M			0.58	0.56	0.54	0.60
CEDRO25M			0.40	0.38	0.61	0.54
CEDRO15M			0.64	0.56	0.53	0.57
CEDRO26M			0.55	0.42	0.49	0.55
CEDRO90M			0.45	0.53	0.50	0.48
CEDRO22M			0.46	0.26	0.33	0.44
CEDRO50M			0.60	0.53	0.36	0.44
CEDRO13M				0.33	0.46	0.37
CEDRO21M				0.46	0.55	0.46
CEDRO4MV				0.07	0.24	0.20
CEDRO20M				0.43	0.55	0.47
CEDRO23M				0.43	0.24	0.50
CEDRO70M					0.57	0.62

In order to eliminate the impact of biological factors on tree-ring growth pattern, the raw tree-ring series were detrended and standardized, and the residual master chronology was built [60]. Figure 5 shows the standard chronology using Tuckey's biweight robust mean [69] and the residual chronology using the residuals of an AR process. Values presented are the dimensionless ring-width index (RWI) and the sample depth over time.

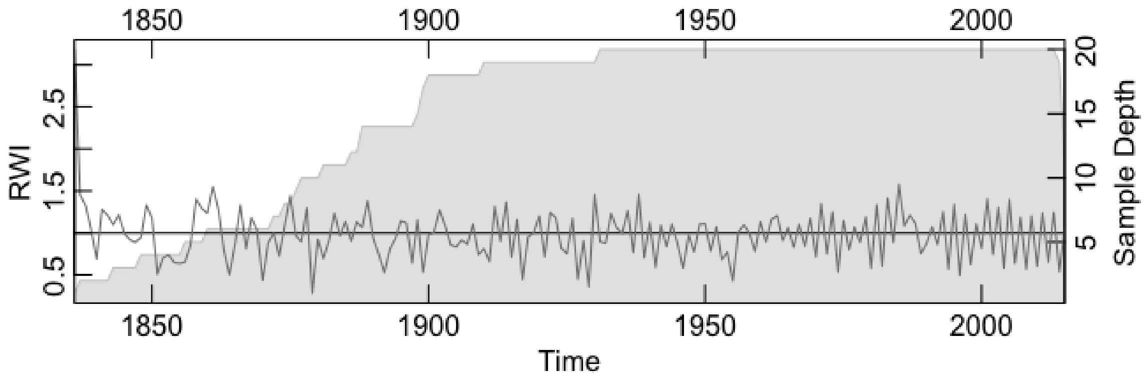

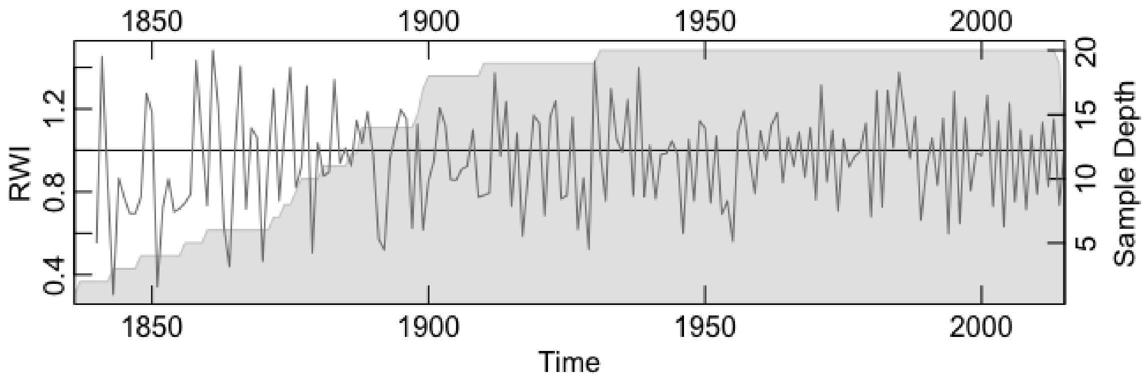

Figure 5. Standard chronology (**above**) and residual chronology (**below**).

The chronology showed an overall EPS of 0.827 and an overall rbt of 0.193. For building a chronology, Wigley, Briffa, and Jones [56] recommend an EPS threshold value of 0.85, which is slightly higher than the EPS realized in our data. However, the threshold recommendation is rather arbitrary and has fallen short in other studies [10].

3.2. Impact of Precipitation and El Niño on Tree Growth

Monthly precipitation and the climate indices Niño 1 + 2 (Extreme Eastern Tropical Pacific SST), Niño 3 .4 (East Central Tropical Pacific SST), MEI (Multivariate ENSO Index), SOI (Southern Oscillation Index), NAO (Northern Atlantic Oscillation), TNA (Tropical North Atlantic Index), and TSA (Tropical South Atlantic Index) values from January of the previous year to December of the current year were used as predictors of tree growth to calculate response and correlation functions by applying the function dcc of the R-package treeclim [66].

When considering the entire time series, a significant influence on annual ring formation was found for the precipitation of the months August of the previous year, as well as of the months June and August of the current year. Thus, not only the precipitation in the respective year under consideration, but also the precipitation of the previous year has an influence on the formation of annual rings. With the exception of SOI, for all ENSO indices, months with a significant influence on annual ring growth were found (Table 2).

Table 2. Precipitation and ENSO indices.

Month		**Precipitation**	**Index**						
			Niño 1 + 2	**Niño 3 .4**	**MEI**	**SOI**	**NAO**	**TSA**	**TNA**
Previous year	January								
	February								
	March							X	
	April							X	
	May								
	June						X	X	X
	July								X
	August	X						X	
	September			X					
	October		X					X	
	November		X					X	
	December		X						
Current year	January				X				
	February							X	X
	March								
	April								
	May				X				
	June	X							
	July			X					
	August	X					X		
	September								
	October								
	November								
	December								

X: significant at $p < 0.05$.

4. Discussion

We present the first tree-ring chronology for *C. odorata* on the Guiana Shield. The growth period shown in the tree rings extends from October of the previous year to August of the current year. The growth of the trees is interrupted by the long, dry season from mid-August to October. A first question was whether the monthly rainfall and the SSTAs are related to the tree-ring widths of the trees investigated. For our dataset, we found dependencies of annual tree ring growth on precipitation in the months June and August of the current year and August of the previous year, thus indicating the influence of the amount of precipitation in the current long, wet season, i.e., at the beginning and during the month with the highest precipitation. Since the trees grow mainly during the rainy season, these dependencies are obvious. However, what explains the dependence on precipitation in August of the previous year? The amount of precipitation in August determines the length of the long, wet season and causes higher soil water potential and water storage in the stem of trees [49]. Some tropical deciduous tree species such a *C. odorata* shed the leaves in response to rainfall reduction during the dry season to establish high solute content and high water potential of stem tissue as prerequisites for flowering and bud break during drought [70,71]. Our results correspond to findings from other studies on *C. ordorata* in Brazilian wet tropical forest [50], as well as dry tropical forest in Venezuela [49] and in Bolivia [25]. Dünisch Bauch, and Gasparotto [50] explained this high sensitivity of *C. odorata* to soil water potential by the root system in the upper soil.

Nurmohamed, Naipal, and Becker [4] studied the influence of sea surface temperature anomalies (SSTAs) in the tropical Atlantic and the tropical Pacific on the seasonal distribution of precipitation in Suriname. They showed that the rainfall anomalies are fairly evenly distributed throughout the country. In the short, wet season (December to January) and the beginning of the long, wet season (March to May), they found the strongest correlation with the SSTAs in the Pacific region (Niño 1 + 2 at a lag of 1 month and Niño 1 + 2 at a lag of 3 months, respectively). For the rainfall in the end part of the long, wet season (June to August) and in the long, dry season (September to November), they observed correlations with the SSTAs in the tropical south Atlantic (TSA at a lag of 0 months and TSA at a lag of 3 months, respectively). They explained the spatial and temporal variability of precipitation by the meridional movement of the ITCZ. The rainfall from August to December of the previous year determines the end of the long, wet season, the length of the long, dry season, and the beginning of the short, wet season. This explains the connection with the SSTAs of the tropical Pacific (Niño 1 + 2 and Niño 3 .4) and the tropical South Atlantic (TSA). The SSTAs of the tropical Atlantic from February to April determine the end of the short, wet season, the length and precipitation of the short, dry season, and the beginning of the long, wet season, which explains the dependencies of the annual tree-ring growth on the TSA and TNA of the respective months. The precipitation in the long, wet season of the previous year again determines the higher soil water potential and water storage in the stem of trees and is reflected in the dependencies on NAO, TSA, and TNA. Thus, the direct dependence of the increase in the precipitation distribution can be transferred to the SSTAs. This provides the basis for the growth of the annual ring to be dependent on El Niño events.

Commonly, anomalies of local conditions related to El Niño events, such as flood pulse [7], precipitation [7,8,12], or drought events [9,15,19] are used to derive the influence of El Niño on annual growth. Rodriguez, Mabres, Luckman, Evans, Masiokas, and Ektvedt [8] found a negative correlation of ring width with a mean November–April Southern Oscillation Index (SOI). We applied a dendroclimatic approach directly to various ENSO indices to derive dependencies on annual tree growth.

5. Conclusions

Our study suggests that the annual tree-ring growth of *C. odorata* is influenced by the climate and, thus, provides further evidence for the annual nature of growth rings for trees growing in the Neotropics. Using ENSO indices allows analyses to be carried out independently of local weather recordings, thus significantly expanding the use of existing datasets to describe tree growth. In addition, the importance of dendroclimatology for the study of the impacts of climate change on tropical forest ecosystems could once again be demonstrated.

Author Contributions: M.K. and N.L. conceptualized and designed the study; M.K. and N.L. collected samples from the field; N.L. conducted lab work; M.K., N.L. and A.G. analyzed data, interpreted results, and wrote the manuscript. All authors have read and agreed to the published version of the manuscript.

Funding: This research was partially funded by the Deutsche Forschungsgemeinschaft (DFG, German Research Foundation) under Germany's Excellence Strategy—EXC 2037 'CLICCS—Climate, Climatic Change, and Society'—Project Number: 390683824, contribution to the Center for Earth System Research and Sustainability (CEN) of Universität Hamburg.

Institutional Review Board Statement: Not applicable.

Informed Consent Statement: Not applicable.

Data Availability Statement: All data relevant to the study are included in the article.

Acknowledgments: We thank Philip Mundhenk, Universität Hamburg–World Forestry, for comments on the manuscript and for valuable hints on R programming and Rewiechand Matai, Stichting Bosbeheer en Bostoezicht, Paramaribo, Suriname, for making the tree samples and Suriname's national record of logged trees available. We also thank Schweingruber (†) and O.U. Bräker for previous extended discussions on tree-ring analyses. We also specially thank Sabine Kruse for her unremitting support during the lab analyses.

Conflicts of Interest: The authors declare no conflict of interest.

References

1. Hall, T.C.; Sealy, A.M.; Stephenson, T.S.; Kusunoki, S.; Taylor, M.A.; Chen, A.A.; Kitoh, A. Future climate of the Caribbean from a super-high-resolution atmospheric general circulation model. *Theor. Appl. Climatol.* **2013**, *113*, 271–287. [CrossRef]
2. Collins, M.; An, S.-I.; Cai, W.; Ganachaud, A.; Guilyardi, E.; Jin, F.-F.; Jochum, M.; Lengaigne, M.; Power, S.; Timmermann, A.; et al. The impact of global warming on the tropical Pacific Ocean and El Nino. *Nat. Geosci.* **2010**, *3*, 391–397. [CrossRef]
3. Walsh, K.J.E.; McInnes, K.L.; McBride, J.L. Climate change impacts on tropical cyclones and extreme sea levels in the South Pacific—A regional assessment. *Glob. Planet. Change* **2012**, *80*, 149–164. [CrossRef]
4. Nurmohamed, R.; Naipal, S.; Becker, C. Rainfall variability in Suriname and its relationship with the Tropical Pacific ENSO SST anomalies and the Atlantic SST anomalies. *Acta Nova* **2006**, *3*, 488–502. [CrossRef]
5. Mol, J.H.; Resida, D.; Ramlal, J.S.; Becker, C.R. Effects of El nino-related drought on freshwater and brackish-water fishes in suriname, South America. *Environ. Biol. Fishes* **2000**, *59*, 429–440. [CrossRef]
6. Iizumi, T.; Luo, J.-J.; Challinor, A.J.; Sakurai, G.; Yokozawa, M.; Sakuma, H.; Brown, M.E.; Yamagata, T. Impacts of El Niño Southern Oscillation on the global yields of major crops. *Nat. Commun.* **2014**, *5*, 3712. [CrossRef] [PubMed]
7. Schöngart, J.; Junk, W.J.; Piedade, M.T.F.; Ayres, J.M.; Hüttermann, A.; Worbes, M. Teleconnection between tree growth in the Amazonian floodplains and the El Nino–Southern Oscillation effect. *Glob. Change Biol.* **2004**, *10*, 683–692. [CrossRef]
8. Rodriguez, R.; Mabres, A.; Luckman, B.; Evans, M.; Masiokas, M.; Ektvedt, T.M. "El Niño" events recorded in dry-forest species of the lowlands of northwest Peru. *Dendrochronologia* **2005**, *22*, 181–186. [CrossRef]
9. Gebrekirstos, A.; Mitlöhner, R.; Teketay, D.; Worbes, M. Climate–growth relationships of the dominant tree species from semi-arid savanna woodland in Ethiopia. *Trees* **2008**, *22*, 631. [CrossRef]
10. De Ridder, M.; Toirambe, B.; van den Bulcke, J.; Bourland, N.; van Acker, J.; Beeckman, H. Dendrochronological Potential in a Semi-Deciduous Rainforest. The Case of Pericopsis elata in Central Africa. *Forests* **2014**, *5*, 3087–3106. [CrossRef]
11. Hofhansl, F.; Kobler, J.; Ofner, J.; Drage, S.; Polz, E.M.; Wanek, W. Sensitivity of tropical forest aboveground productivity to climate anomalies in SW Costa Rica. *Glob. Biogeochem. Cycles* **2014**, *28*, 1437–1454. [CrossRef]
12. Moreno, M.M.; del Valle, J.I. Influence of local climate and ENSO on the growth of Abarco (*Cariniana pyriformis*) in Choc, Colombia. *Trees* **2015**, *29*, 97–107. [CrossRef]
13. Rozas, V.; Camarero, J.J.; Sanguesa-Barreda, G.; Souto, M.; Garcia-Gonzalez, I. Summer drought and ENSO-related cloudiness distinctly drive Fagus sylvatica growth near the species rear-edge in northern Spain. *Agric. For. Meteorol.* **2015**, *201*, 153–164. [CrossRef]
14. Perone, A.; Lombardi, F.; Marchetti, M.; Tognetti, R.; Lasserre, B. Evidence of solar activity and El Nino signals in tree rings of *Araucaria araucana* and *A. angustifolia* in South America. *Glob. Planet. Change* **2016**, *145*, 1–10. [CrossRef]

15. Spannl, S.; Volland, F.; Pucha, D.; Peters, T.; Cueva, E.; Bräuning, A. Climate variability, tree increment patterns and ENSO-related carbon sequestration reduction of the tropical dry forest species Loxopterygium huasango of Southern Ecuador. *Trees* **2016**, *30*, 1245–1258. [CrossRef]
16. Venegas-Gonzalez, A.; Chagas, M.P.; Anholetto, C.R.; Alvares, C.A.; Roig, F.A.; Tomazello, M. Sensitivity of tree ring growth to local and large-scale climate variability in a region of Southeastern Brazil. *Theor. Appl. Climatol.* **2016**, *123*, 233–245. [CrossRef]
17. Alfaro-Sanchez, R.; Muller-Landau, H.C.; Wright, S.J.; Camarero, J.J. Growth and reproduction respond differently to climate in three Neotropical tree species. *Oecologia* **2017**, *184*, 531–541. [CrossRef]
18. García-Cervigón, A.I.; Camarero, J.J.; Espinosa, C.I. Intra-annual stem increment patterns and climatic responses in five tree species from an Ecuadorian tropical dry forest. *Trees* **2017**, *31*, 1057–1067. [CrossRef]
19. Berenguer, E.; Malhi, Y.; Brando, P.; Cardoso Nunes Cordeiro, A.; Ferreira, J.; Franca, F.; Chesini Rossi, L.; Maria Moraes de Seixas, M.; Barlow, J. Tree growth and stem carbon accumulation in human-modified Amazonian forests following drought and fire. *Phil. Trans. R. Soc. B* **2018**, *373*, 20170308. [CrossRef]
20. Köhl, M.; Scott, C.T.; Zingg, A. Evaluation of Permanent Sample Surveys for Growth and Yield Studies. *For. Ecol. Manag.* **1995**, *71*, 187–194. [CrossRef]
21. Nagel, J.; Spellmann, H.; Pretzsch, H. Zum Informationspotenzial langfristiger forstlicher Versuchsflächen und periodischer Waldinventuren für die waldwachstumskundliche Forschung. *Allg. Forst-Und Jagdztg.* **2012**, *183*, 111–116.
22. Lutz, J.A. The Evolution of Long-Term Data for Forestry: Large Temperate Research Plots in an Era of Global Change. *Northwest Sci.* **2015**, *89*, 255–269. [CrossRef]
23. Fritts, H.C. *Tree Rings and Climate*; Academic Press: London, UK, 1976.
24. Schweingruber, F. *Tree Rings: Basics and Applications of Dendrochronology*; Springer: Berlin/Heidelberg, Germany, 2007.
25. Brienen, R.J.; Zuidema, P.A. Relating tree growth to rainfall in Bolivian rain forests: A test for six species using tree ring analysis. *Oecologia* **2005**, *146*, 1–12. [CrossRef]
26. Garcıa-Suárez, A.M.; Butler, C.J.; Baillie, M.G.L. Climate signalintree-ringchronologiesinatemperateclimate: A multi-speciesapproach. *Dendrochronologia* **2009**, *27*, 183–190. [CrossRef]
27. Van der Sleen, P.; Groenendijk, P.; Vlam, M.; Anten, N.P.R.; Bongers, F.; Zuidema, P.A. Trends in tropical tree growth: Re-analyses confirm earlier findings. *Glob. Change Biol.* **2017**, *23*, 1761–1762. [CrossRef] [PubMed]
28. Lindner, M.; Maroschek, M.; Netherer, S.; Kremer, A.; Barbati, A.; Garcia-Gonzalo, J.; Seidl, R.; Delzon, S.; Corona, P.; Kolstrom, M.; et al. Climate change impacts, adaptive capacity, and vulnerability of European forest ecosystems. *For. Ecol. Manag.* **2010**, *259*, 698–709. [CrossRef]
29. Hanewinkel, M.; Cullmann, D.A.; Schelhaas, M.J.; Nabuurs, G.J.; Zimmermann, N.E. Climate change may cause severe loss in the economic value of European forest land. *Nat. Clim. Change* **2012**, *3*, 203–207. [CrossRef]
30. Lamprecht, H. *Silviculture in the Tropics: Tropical Forest Ecosystems and Their Tree Species. Possibilities and Methods for Their Long Term Utilization*; GIZ: Eschborn, Germany, 1989.
31. Newberry, D.M.; Ridsdale, W.E. Neighbourhood abundance and small-tree survival in a lowland Borneam rainforest. *Ecol. Res.* **2016**, *31*, 353–366. [CrossRef]
32. Nguyen, H.H.; Uria-Diez, J.; Wiegand, K. Spatial distribution and association patterns in a tropical evergreen broad-leaved forest of north-central Vietnam. *J. Veg. Sci.* **2016**, *27*, 318–327. [CrossRef]
33. Rodrigues, D.R.; Bovolenta, Y.R.; Pimenta, J.A.; Bianchini, E. Height structure and spatial pattern of five tropical tree species in two seasonal semideciduous forest fragments with different conservation histories. *Rev. Arvore* **2016**, *40*, 395–405. [CrossRef]
34. Le Bec, J.; Courbaud, B.; Le Moguédec, G.; Pélissier, R. Characterizing tropical tree species growth strategies: Learning from inter-Individual variability and scale invariance. *PLoS ONE* **2015**, *10*, e0117028. [CrossRef] [PubMed]
35. Rapp, J.M.; Silman, M.R.; Clark, J.S.; Girardin, C.A.J.; Galiano, D.; Tito, R. Intra- and interspecific tree growth across a long altitudinal gradientin the Peruvian Andes. *Ecology* **2012**, *93*, 2061–2072. [CrossRef] [PubMed]
36. Yoda, K.; Shinozaki, K.; Ogawa, H.; Hozumi, K.; Kira, T. Estimation of the total amount of respiration in woody organs of trees and forest communities. *J. Biol. Osaka City Univ.* **1965**, *16*, 15–26.
37. Whittaker, R.H.; Woodwell, G.M. Surface area relations of woody plants and forest communities. *Am. J. Botany* **1967**, *54*, 931–939. [CrossRef]
38. Coombs, J.; Hall, D.O.; Long, S.P.; Scurlock, J.M.O. *Techniques in Bioproductivity and Photosynthesis*, 2nd ed.; Pergamon: Oxford, UK, 1985.
39. Ryan, M.G.; Phillips, N.; Bond, B.J. The hydraulic limitation hypothesis revisited. *Plant Cell Environ.* **2006**, *29*, 367–381. [CrossRef]
40. Woodruff, D.R.; Meinzer, F.C. Size-dependent changes in biophysical control of tree growth: The role of turgor. In *Size- and Age-Related Changes in Tree Structure and Function*; Meinzer, F.C., Lachenbruch, B., Dawson, T.E., Eds.; Springer: Dordrecht, The Netherlands, 2011; Tree Physiology; Volume 4, pp. 363–384.
41. Ryan, M.G.; Yoder, B.J. Hydraulic limits to tree height and tree growth. *BioScience* **1997**, *47*, 235–242. [CrossRef]
42. Worbes, M. One hundred years of tree-ring research in the tropics—A brief history and an outlook to future challenges. *Dendrochronologia* **2002**, *20*, 217–231. [CrossRef]
43. Lotfiomran, N.; Köhl, M. Retrospective analysis of growth: A contribution to sustainable forest management in the tropics. *IAWA J.* **2017**, *38*, 297-S221. [CrossRef]
44. FAO. *Global Forest Resources Assessment 2015*; FAO: Rome, Italy, 2015.

45. Werger, M.J.A. *Sustainable Management of Tropical Rainforests—The CELOS Management System*; Tropenbos International: Paramaribo, Suriname, 2011; p. 281.
46. Rayner, N.A.; Parker, D.E.; Horton, E.B.; Folland, C.K.; Alexander, L.V.; Rowell, D.P.; Kent, E.C.; Kaplan, A. Global analyses of sea surface temperature, sea ice, and night marine air temperature since the late nineteenth century. *J. Geophys. Res.* **2003**, *108*, 4407. [CrossRef]
47. Burns, R.M.; Honkala, B.H. *Silvics of North America: U.S.D.A. Forest Service Agriculture Handbook 654*; Forest Service, United States Department of Agriculture: Washington, DC, USA, 1990.
48. IUCN. *The IUCN Red List of Threatened Species*; Version 2015-4; International Union for Conservation of Nature: Gland, Switzerland, 2016. Available online: http://www.iucnredlist.org (accessed on 23 May 2016).
49. Worbes, M. Annual growth rings, rainfall-dependent growth and long-term growth patterns of tropical trees from the Caparo Forest Reserve in Venezuela. *J. Ecol.* **1999**, *87*, 391–403. [CrossRef]
50. Dünisch, O.; Bauch, J.; Gasparotto, L. Formation of increment zones and intraannual growth dynamics in the xylem of Swietenia Macrophylla, Carapa guianensis, and Cedrela odorata (Meliaceae). *IAWA J.* **2002**, *23*, 101–119. [CrossRef]
51. Worbes, M. How to measure growth dynamics in tropical trees—A review. *IAWA J.* **1995**, *16*, 337–351. [CrossRef]
52. Rinn, F. *LINTAB 6 Tree-Ring Measurement Station*; Rinntech: Heidelberg, Germany.
53. Rinn, F. *TSAP-Win—Time Series Analysis and Presentation Dendrochronology and Related Applications*; Rinntech: Heidelberg, Germany, 2003.
54. Stokes, M.A.; Smiley, T.L. *An Introduction to Tree-Ring Dating*; University of Arizona Press: Tucson, AZ, USA, 1996.
55. Briffa, K.R.; Jones, P.D. Basic chronology statistics and assessment. In *Methods of Dendrochronology: Applications in the Environmental Sciences*; Kluwer Academic Publishers: Dordrecht, The Netherlands, 1990.
56. Wigley, T.M.; Briffa, K.R.; Jones, P.D. On the average value of correlated time series, with applications in dendroclimatology and hydrometeorology. *J. Clim. Appl. Meteorol.* **1984**, *23*, 201–213. [CrossRef]
57. Eckstein, D.; Bauch, J. Beitrag zur Rationalisierung eines dendrochronologischen Verfahrens und zur Analyse seiner Aussagesicherheit. *Forstwiss. Centralblatt* **1969**, *88*, 230–250. [CrossRef]
58. Baillie, M.; Pilcher, J. A simple cross-dating program for tree-ring research. *Tree-Ring Bull.* **1973**, *38*, 35–43.
59. Holmes, R.L. Computer-assisted quality control in tree-ring dating and measurement. *Tree-Ring Bull.* **1983**, *44*, 69–75.
60. Bunn, A.; Korpela, M.; Biondi, F.; Campelo, F.; Mérian, P.; Qeadan, F.; Zang, C. DplR: Dendrochronology Program Library in R. R Package Version 1.6.5. 2017. Available online: https://CRAN.R-project.org/package=dplR (accessed on 14 June 2022).
61. Cook, E.; Peters, K. The smoothing spline: A new approach to standardizing forest interior tree-ring width series for dendroclimatic studies. *Tree-Ring Bull.* **1980**, *41*, 45–53.
62. Bunn, A.G. Statistical and visual crossdating in R using the dplR library. *Dendrochronologia* **2010**, *28*, 251–258. [CrossRef]
63. R Core Team. *R: A Language and Environment for Statistical Computing*; R Foundation for Statistical Computing: Vienna, Austria, 2017.
64. Guiot, J. The bootstrapped response function. *Tree Ring Bull.* **1991**, *51*, 39–41.
65. Zang, C.; Biondi, F. Dendroclimatic calibration in R: The bootRes package for response and correlation function analysis. *Dendrochronologia* **2013**, *31*, 68–74. [CrossRef]
66. Zang, C.; Biondi, F. treeclim: An R package for the numerical calibration of proxy-climate relationships. *Ecography* **2015**, *38*, 431–436. [CrossRef]
67. Garcia-Gonzalo, J.; Peltola, H.; Briceño-Elizondo, E.; Kellomäki, S. Effects of climate change and management on timber yield in boreal forests, with economic implications: A case study. *Clim. Change* **2007**, *81*, 431–454. [CrossRef]
68. Brienen, R.J.W.; Gloor, M.; Ziv, G. Tree demography dominates long-term growth trends inferred from tree rings. *Glob. Change Biol.* **2017**, *23*, 474–484. [CrossRef] [PubMed]
69. Wilcox, R. *Introduction to Robust Estimation and Hypothesis Testing*; Elsevier: Burlington, MA, USA, 2005.
70. Borchert, R. Climatic periodicity, phenology, and cambium activity in tropical dry forest trees. *IAWA J.* **1999**, *20*, 239–247. [CrossRef]
71. Sauter, J. Photosynthate allocation of the vascular cambium: Facts and problems. In *Cell and Molecular Biology of Wood Formation*; Savidge, R.A., Barnett, J.R., Napier, R., Eds.; BIOS Scientific: Oxford, UK, 2000; pp. 71–84.